Forest and Society
Vol. 6(1): 355-377, April 2022
http://dx.doi.org/10.24259/fs.v6i1.18271

REGULAR RESEARCH ARTICLE

Impact of Climate Change and Variability on Spatiotemporal Variation of Forest Cover; World Heritage Sinharaja Rainforest, Sri Lanka

Jayanga T. Samarasinghe[1], Miyuru B. Gunathilake[2], Randika K. Makubura[3], Shanika M.A. Arachchi[4], and Upaka Rathnayake[3],*

AFILIATIONS

1. Department of Earth Environmental and Resource Sciences, University of Texas, El Paso, USA
2. Hydrology and Aquatic Environment, Division of Environment and Natural Resources, Norwegian Institute of Bioeconomy and Research, Ås, Norway
3. Department of Civil Engineering, Faculty of Engineering, Sri Lanka Institute of Information Technology, Malabe, Sri Lanka
4. Department of Applied Computing, Faculty of Computing and Technology, University of Kelaniya, Kelaniya, Sri Lanka

Correspondence:
upakasanjeewa@gmail.com

RECEIVED 2021-07-09
ACCEPTED 2022-03-24

ABSTRACT

Rainforests are continuously threatened by various anthropogenic activities. In addition, the ever-changing climate severely impacts the world's rainforest cover. The consequences of these are paid back to human at a higher cost. Nevertheless, little or no significant attention was broadly given to this critical environmental issue. The World Heritage Sinharaja Rainforest in Sri Lanka is originating news on its forest cover due to human activities and changing climates. The scientific analysis is yet to be presented on the related issues. Therefore, this paper presents a comprehensive study on the possible impact on the Sinharaja Rainforest due to changing climate. Landsat images with measured rainfall data for 30 years were assessed and the relationships are presented. Results showcased that the built-up areas have drastically been increased over the last decade in the vicinity and the declared forest area. The authorities found the issues are serious and a sensitive task to negotiate in conserving the forest. The rainfall around the forest area has not shown significant trends over the years. Therefore, the health of forest cover was not severely impacted. Nevertheless, six cleared-up areas were found inside the Singaraja Rainforest under no human interactions. This can be due to a possible influence from the changing climate. This was justified by the temporal variation of Land Surface Temperature (LST) assessments over these six cleared-up areas. Therefore, the World Heritage rainforest is threatened due to human activities and under the changing climate change. Hence, the conservation of the Sinharaja Rainforest would be challenging in the future.

KEYWORDS

Climate change and variability; forest cover; Landsat; rainfall; Land Surface Temperature (LST); Sinharaja rainforest

1. INTRODUCTION

World forest cover has been drastically reduced over time. This could be due to natural reasons like landslides, avalanches, snow breakages, wind throws, fires and insect outbreaks (Bebi et al., 2017). However, the natural causes can be considered minor factors for deforestation compared to human activities over time. Population increase has continuously increased the rate of urbanization (Leach & Fairhead, 2000; Wang et al., 2020) and the forest areas are being threatened. In addition, forest areas are continuously deforested to satisfy the rising food demand of the people (Gibbs et al., 2010). Therefore, agriculture is a major factor in the decreasing forest cover, and there are enough examples from the past (Birhane et al., 2019; Heartsill-Scalley & Aide, 2003; Temudo & Silva, 2012; Zhu & Waller, 2003).

The agriculture and development projects, like construction of new reservoirs (Benchimol & Peres, 2015; Chen et al., 2019), expressways (Ji et al., 2014), etc. have reduced the forest cover significantly. The forest cover in Sri Lanka is following the same trends, which can be seen for the world with agriculture and development

projects (Ranagalage et al., 2020; Rathnayake et al., 2020). Lindström et al. (2012) have investigated the forest cover change in Sri Lanka for two conserved natural forests (naming Kanneliya forest reserve and Knuckles conservation forest) due to the small farming activities. Results revealed a significant forest cover decrease in the Kanneliya forest reserve, whereas a considerable increase in the Knuckles conservation forest (due to the imposed rules and regulations). In general, Ranagalge et al. (2020) have found a significant decrease in the forest cover in Sri Lanka over the years and that could well be due to human activities. Nevertheless, very little research work has been carried out in the context of Sri Lanka to identify the localized forest cover change.

Climate change and forest cover reduction are two interconnected activities. When there is an ongoing climate change, the forest cover is naturally impacted and vice versa. The land-use and land cover changes (LULCC) cause a significant impact on regional climates over regional and global scales (Sy & Quesada, 2020). Thus, the LULCC impacts lead to change the ecosystems and then, to change the global climates. Margono et al. (2014) stated that greenhouse gas emissions were observed due to clearing the primary forest areas in Indonesia. In addition, significant biodiversity loss was observed in the process. For 12 years (2000 to 2012), they have quantified a loss of 6.02 Mha, higher than that of Brazil.

Choi et al. (2011) have showcased a prediction model to identify the forest cover changes in South Korea. They have used the hydrological and thermal indices in their prediction model. In addition, a prediction model based on the climate scenarios for Europe was developed by Härkönen et al. (2019). The relationship between climate change and forest cover change has well been addressed in many areas in the world. However, no or very limited research has been carried out along the lines of climate change and forest cover (as per the authors' knowledge) in the context of Sri Lanka.

Analyzing the temporal variation of the forest cover has been a demanded topic in the research world. Many researchers have used time-dependent satellite images to analyze forest cover change. Landsat satellite imageries from 1990 to 2000 were used to analyze the forest cover change in one of the most forested countries in Southeast Asia, Myanmar by Leimgruber et al. (2005). Their analysis showcased the importance of the forest cover on biodiversity and found a rate of 0.3% annual forest cover declination. Similar analysis can be found in the literature for many other countries and areas (Huang et al., 2009; Kim et al., 2011; Stibig & Malingreau, 2003). These Landsat satellite images can sometimes be incomplete for various reasons, including the climate effects, satellite resolutions, and cloud cover. Khan et al. (2017) have incorporated a deep neural network to overcome some of the issues in incomplete satellite images for forest cover detection. A similar technique was used in much other research work to overcome some of the issues in satellite images and enhance the quality of the research work (Kislov et al., 2021; Sylvain et al., 2019). The forest covers in some of the areas of Sri Lanka were assessed by several researchers (Lindström et al., 2012; Perera & Tsuchiya, 2009; Rathnayake et al., 2020). However, none showcased a depth and detailed analysis of the World Heritage Rainforest, Sinharaja.

Sinharaja Rainforest is a World Heritage site in Sri Lanka and faced many anthropogenic activities over the recent past and threatened its forest cover and its biodiversity. Many development activities in the circumference of the Sinharaja Rainforest have happened in the recent past and local and international environmentalists have strongly showcased the importance of protecting this World Heritage. However, there are many drawbacks to the conservation of World Heritage.On the other hand, no research can be found to showcase the temporal variation of the forest cover over the years in the Sinharaja Rainforest due to anthropogenic activities and to change climate. Therefore, the research world has no scientific information on

the forest cover in Sinharaja Rainforest. To overcome the showcased research gap, this research presents novel research work on this World Heritage Sinharaja Rainforest cover to analyze the temporal variation of the forest cover and its relationships to the surface temperatures. Promising results are found from this study, and these results can effectively be used in a comprehensive conservation program of Sinharaja Rainforest, Sri Lanka.

2. STUDY AREA

Sinharaja Rainforest Reserve is located in southwest Sri Lanka and is considered the last extensive patch of primary lowland tropical rainforest in Sri Lanka, covering approximately an area of 8,864 ha. The forest can be seen at an altitude of 300 m – 1,170 m. The reserve consists of 6,092 ha of forest coverage. In addition, another 2,772 ha are proposed for the reserve. The forest reserve is within the latitude of 60 21' and 60 26' North and longitude of 800 21' and 800 34' East (refer Figure 1); therefore, it bounds to Rathnapura, Galle, and Matara districts of Sri Lanka.

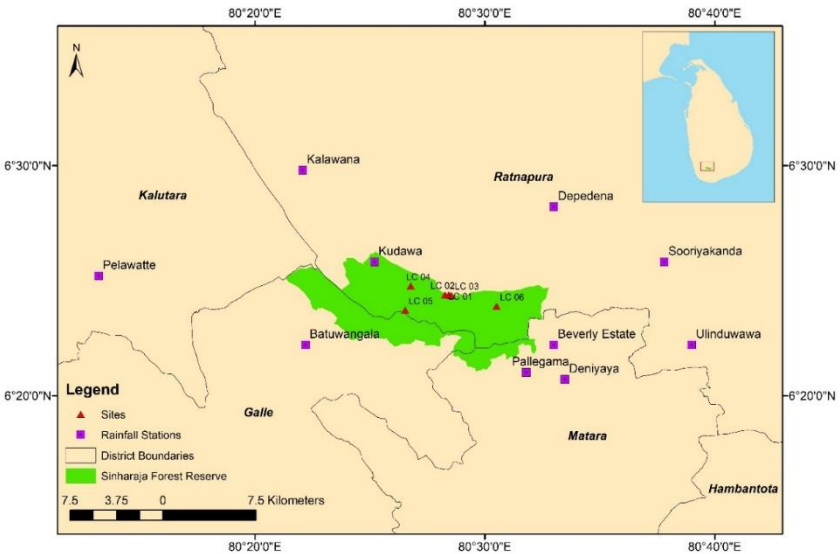

Figure 1. Study area with rainfall gauges and observed damaged sites

The area was first declared as a forest reserve in 1875. At that time, the Sinharaja Rainforest reserve had an area of about 23,000 ha (Baker, 1937), The area was reduced to 8,864 ha with some human settlements inside the declared forest area. Extensive logging was continued until 1978. This has caused severe damage to the ecosystem of the Sinharaja Rainforest. The National Heritage Wilderness Act presented in 1988 helped to ban the logging and replantation of logged areas.

The forest covers two important geological zones including the South-western and Highland groups. In addition, the mean annual rainfall to the forest area is around 3750 mm to 5000 mm. The rainy season activates in the south-western and north-eastern monsoon times. A total of 139 (64%) out of 217 trees and woody climbers, which are endemic species in the lowland of Sri Lanka, and can be found in the Sinharaja Rainforest (Examples: Humboldtia laurufolia, Elaeocarpus Coriaceus, Uncria Thwatesii, Litcea Longifolia, etc.). In addition, 19 out of 20 endemic Sri Lankan birds can be found in reserve (Examples: Green – Billed Coucal, Small Miniver, Yellow-Broed Bulbul, The Sri Lanka Blue Magpie, etc.). Endemic butterflies count is more than 50%

inside the reserve. Furthermore, threatened mammals like black leopards and Indian elephants can also be seen in the forest. Therefore, the forest reserve was named as a UNESCO World Heritage site in 1987 (Gunathilake et al., 1987). Nevertheless, the forest reserve is under serious threat due to the population increase, new settlements, infrastructure development, cultivations, etc. Therefore, there are many critical reviews (especially in the local newspaper in Sri Lanka) on the moving boundaries of the Sinharaja rainforest reserve.

3. MATERIALS AND METHODS

3.1. Climatic and remote sensing data

The Forest boundary for the Sinharaja rainforest according to the 2012 publication was obtained from United Nations Educational, Scientific and Cultural Organization (UNESCO) (https://en.unesco.org/). The required climatic data were purchased from the Department of Meteorology, Sri Lanka. The monthly cumulative rainfall data for the rainfall stations around the Sinharaja Rainforest were obtained for 30 years (from 1989 to 2019) for Kudawa, Deniyaya, Pallegamathanna, Pelawatta, and Depedena rainfall stations. In addition, monthly rainfall data for 3 years (from 2016 – 2019) from newly established rainfall stations, including Batuwangala, Breverly Estate, Sooriyakanda, Kalawana, and Ulinduwawa were purchased. The spatial distribution of the rainfall stations around the Sinharaja rainforest can be seen in Figure 1.

Furthermore, the daily minimum and maximum atmospheric temperatures and morning and evening relative humidities of Deniyaya for some of the selected months (March 1992, April 1995, February 1997, February 2005, February 2016, and February 2019) were purchased from the Department of Meteorology, Sri Lanka. In addition, measured land surface temperature data (5 cm below the surface) for Matara for some of the selected dates were obtained from the Department of Agriculture, University of Ruhuna, Sri Lanka. Moreover, the satellite images for image processing were obtained from USGS Earth Explorer at https://earthexplorer.usgs.gov/ for Landsat 5 Thematic Mapper (for the years 1992 – 2005), Landsat 8 Operational Land Imager (for the years 2016 – 2019), and Google Earth Pro (for the years 2001 – 2019).

3.2. Landsat image extraction and forest cover detection

Opensource Land observatory missions (i.e., Landsat, Sentinel 2) provide the finest resolution of satellite images ranging from 15-30 m (to maintain homogeneity, Landsat images were used for this study) (Fokeng et al., 2020). All these Landsat images are in the raster format. Usually, the commercial satellite missions provide high-resolution images of earth up to 15 cm finest resolution (Jin & Davis, 2007; Zhang et al., 2020). The, 30 m resolution images are widely used and accepted for many applications than high-resolution satellite images (Anderson et al., 2012; Matricardi et al., 2010; van Leeuwen et al., 2011). However, the thermal bands of Landsat images are much coarser than reflective bands.

For this study, the remote-sensed Landsat satellite images from 1992 to 2019 were extracted from Landsat 5 TM and Landsat 8 OLI. The Thematic Mapper (TM) thermal band pixel is about 120 mX120 m in resolution while Operational Land Imager (OLI) thermal band pixel is about 100 mX100 m, respectively. Even though the pixel size is coarser, the land surface temperatures obtained from them are usually acceptable.

Careful consideration was given in selecting the satellite images. Cloud-free or minimum cloud levels (<10%) were extracted for the drier periods.

The images selected during the wet period usually give a large forest cover due to high reflectance in red and near-infrared bands (Fokeng et al., 2020). The satellite images extracted during the wet season were checked and found out that they are

usually with a higher percentage of clouds. This can cause higher reflectance (Sun et al., 2018). Therefore, the images recorded only during the dry period were considered for this study. Table 1 presents a summary of the satellite images extracted for this study.

Table 1. Extracted remote sensing data and ground measurements

Sensor	Extraction for the date of	Spatial Thermal Band Resolution (m) Thermal IR / T1RS 1	T_0 (°C) for Deniyaya	Relative Humidity (RH) (%) for Deniyaya
Landsat 5 TM	13/03/1992	120	25.6	62
	07/04/1995	120	27.7	70
	23/02/1997	120	27.1	78
	13/02/2005	120	25.1	60
Landsat 8 OLI	28/02/2016	100	25.6	62
	20/02/2019	100	27.7	70

Landsat 5 Thermal Band – Band 6
Landsat 8 Thermal Band – Band 10
Spatial resolution (m) Red, Green, Blue – 30 m

The land-use class of the study area was classified with field observations and high-resolution satellite images from Google Earth. The entire classification was conducted for six land-use classes: forests, cultivations, build-ups, water bodies, bare lands, and clouds. The land-use pattern in the defined forest area can be classified with an open-source semi-automated classification plugin in QGIS 3.10 (QGIS is a leading open-source Geographic Information System application), while a supervised classification (using a semi-automated classification tool) was carried out in this study area by training areas and pixel-based image classification. The defined pixels identify the materials in an image according to the material's signatures. Therefore, the land-uses can be identified based on this classification. The semi-automated classification tool was successfully used for this identification. More information on this open-source toolbox can be found in Congedo (2016). In addition, the accuracy assessment of these classifications was conducted with high-resolution images of Google Earth.

The loss or the gain by targeted land-use classes can be calculated by the suggestions from Hansen et al. (2013). In addition, the rate of change of land-uses can be calculated by Equation 1 (Fokeng et al., 2020).

$$Annual\ Change\ Rate\ (ha/year) = \frac{\Delta A}{N} \times 100 \quad (1)$$

where ΔA is the change of area in the targeted land-use class (measured in ha), N is the number of years between the beginning and the end of the study period.

3.3. Land surface temperature (LST) retrieval

Six sites (LC01 – LC06) were selected after carefully observing the forest cover over the years. The high-resolution satellite images were used in these selections and the selected sites are given in Figure 2. Importantly, these sites have deforested or deteriorated forest cover without traceable human interference. There was no clue of gaining the forest back; however, the widening of the deforested area can be observed.

Many researchers suggested several reasons, including increment of surface temperature, implementation of various toxic levels, mortality, etc. were suggested by many researchers for such deforestation inside a forest (Karnieli et al., 2010; Peterson, 2000; Walthert et al., 2013). However, due to the nature of the Sinharaja Rainforest, the increment of surface temperature can be seen as one of the acceptable reasons for such deforestation.

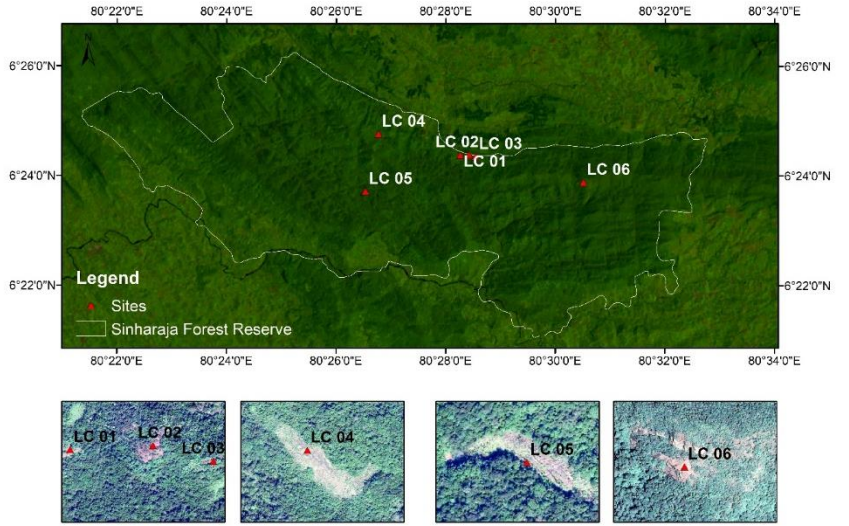

Figure 2. Deforested or deteriorated forest cover sites

Extracted Landsat satellite images were used to estimate the LST of the whole area of the Sinharaja rainforest. These images were segmented in the open-sourced QGIS (https://qgis.org/en/site/) environments using Python programming language. Several methods, including Mono Window Algorithm (MWA) (Athick et al., 2019; Qin et al., 2001), Single Channel Algorithm (SCA) (Chatterjee et al., 2017; Cristóbal et al., 2018; Wang et al., 2016), Radiative Transfer Equation (RTE) (Dash et al., 2001; Yu et al., 2014), and Spilt Window Algorithm (SWA) (Labbi & Mokhnache, 2015; Rongali et al., 2018), can be found in the literature to estimate the LST from the Satellite images.The accuracy of these methods may differ from one to another (García-Santos et al., 2018). Nevertheless, according to the suggestions from Sekertekin & Bonafoni (2020), MWA was used to calculate the land surface temperature in the Sinharaja rainforest. The governing equations for the LST estimation are given in Equations 2-14.

- LST calculations (T_s) (Qin et al., 2001)

$$T_s = \{a.(1 - C - D) + [b.(1 - C - D) + C + D].T - DT_a\} \div C \quad (2)$$

where $a = -67.355351$ and $b = 0.458606$

$$C = \varepsilon \times \tau \quad (3)$$

$$D = (1 - \tau)[1 + (1 - \varepsilon) \times \tau] \quad (4)$$

- Effective mean atmospheric temperature calculations (T_a) (Qin et al., 2001)

$$T_a = 17.977 + 0.9172 \times T_0 \quad \text{(Tropical Region)} \quad (5)$$

where T_0 is the near surface air temperature (*measured in Kelvin*).

- Transmittance calculations (τ_6 and τ_{10})

$$\tau_6 = 1.053710 - 0.14142w \quad \text{- For Landsat 5 (TM)} \quad (6)$$

- The Equation 6 is valid only for the regions with temperatures between 20-30 ^{0}C with a water vapour content (w) between 1.6 – 3.0 (Sekertekin & Bonafoni, 2020).

$$\tau_{10} = -0.0164w^2 - 0.04203w + 0.9715 \quad \text{- For Landsat 8 (OLI)} \tag{7}$$

where w is the water vapour content (g/cm^2).

- Water vapour content calculations (w_i)

$$w_i = 0.0981\left\{10 \times 0.6108\ exp\left[\frac{17.27\ \times (T_0 - 273.15)}{237.3 + (T_0 - 273.15)}\right] \times RH\right\} + 0.1697 \tag{8}$$

- Emissivity calculations (ε) (Sobrino et al., 2008)

$$\varepsilon = \begin{cases} 0.979 - 0.035\rho_R & NDVI < 0.2 \\ 0.004P_v + 0.986 & 0.2 \leq NDVI \leq 0.5 \\ 0.99 & NDVI \geq 0.5 \end{cases} \tag{9}$$

- Normalized Difference Vegetation Index ($NDVI$) calculations (Viana et al., 2019)

$$NDVI = \frac{\rho_{NIR} - \rho_R}{\rho_{NIR} + \rho_R} \tag{10}$$

where ρ_{NIR} is the reflectance band in the NIR region and ρ_R is the reflectance band in the Red region.

- Fractional vegetation cover (P_v) (Song et al., 2017)

$$P_v = \left[\frac{NDVI - NDVI_{MIN}}{NDVI_{MAX} - NDVI_{MIN}}\right]^2 \tag{11}$$

- Radiance (L_λ) calculations (Sekertekin & Bonafoni, 2020)

  Landsat 5 TM (12)

$$L_\lambda = \left[\frac{L_{MAX,\lambda} - L_{MIN,\lambda}}{Q_{CAL,MAX} - Q_{CAL,MAX}}\right] + \left[Q_{CAL} - Q_{CAL,MIN}\right] + L_{MIN,\lambda}$$

  Landsat 8 OLI (13)

$$L_\lambda = M_L Q_{CAL} + A_L$$

where Q_{CAL} is the quantized calibrated pixel value in Digital Number (DN), $L_{MIN,\lambda}$ (Watts/(m^2.srad.μm)) is the spectral radiance scaled to $Q_{CAL,MIN}$, $L_{MAX,\lambda}$ (Watts/(m^2.srad.μm)) is the spectral radiance scaled to $Q_{CAL,MAX}$, $Q_{CAL,MIN}$ is the minimum quantized calibrated pixel value in DN, $Q_{CAL,MAX}$ is the maximum quantized calibrated pixel value in DN, M_L is the band-specific multiplicative rescaling factor, and A_L is the band-specific additive rescaling factor. These values can be obtained from the meta-data file of the Landsat image.

- Brightness Temperature (T) calculations (Mujabar & Rao, 2018)

$$T = \frac{K_2}{\ln\left(\frac{K_1}{L_\lambda} + 1\right)} \tag{14}$$

where K_1 is $607.76\ W/m^2.srad.\mu m$ and K_2 is $1260.56\ K$ for Landsat 5 and K_1 is $774.89\ W/m^2.srad.\mu m$ and K_2 is $1321.08\ K$ for Landsat 8, respectively. The ground

temperature measurements are rare in Sri Lanka. Therefore, such data are scarce. However, the closest real-world ground temperature measurement facility is the Faculty of Agriculture, University of Ruhuna, Sri Lanka, which is around 50 km away was used to validate the estimations.

3.4. Rainfall trend analysis

Rainfall trend analysis were carried out to identify the rainfall trends using the historical rainfall data around the Singharaja forest. The rain gauges used for this study are given in Figure 1. They are well spread around the forest. Thus, it was assumed that the rain gauges around the forest represent the rainfall patterns in the vicinity of the forest. The results of the trends were used to represent any potential impacts to the forest cover.

Purchased monthly rainfall data were used to analyze the rainfall trends. The missing data were filled by the inverse distance method as it is one of the better-suited methods to fill the missing data in the regions of the lower elevated areas (Sirisena & Suriyagoda, 2018), than the other methods (De Silva et al., 2007). Then, the Pettitt's test, SNHT, Buishand's test, and von Neumann's test were carried out to check the homogeneity of the rainfall data series (Haylock et al., 2008; Sahin & Cigizoglu, 2010). Finally, the Mann-Kendall test and Sen's slope estimator tests were carried out to identify any possible rainfall trends.

The Mann–Kendell test is a widely used nonparametric test by many researchers to check the climatic trends (Hirsch & Slack, 1984; Karmeshu, 2012; Khaniya et al., 2019; Mann, 1945; Rathnayake, 2019). Both increasing trends and decreasing trends can be estimated using the Mann–Kendall test by following Equation 15.

$$S = \sum_{i=1}^{n-1} \sum_{j=i+1}^{n} sgn(x_i - x_j) \tag{15}$$

where

$$sgn(x_i - x_j) = \begin{cases} 1 & if\ x_j - x_i > 0 \\ 0 & if\ x_j - x_i = 0 \\ -1 & if\ x_j - x_i < 0 \end{cases}$$

where x_j and x_i are climate data value in months/years j and i here $j > i$. The Mann-Kendall's statistic S is calculated by the Equation 15. The "sgn" sign function is given in the latter part of the equation. However, the Mann–Kendall test is a qualitative measurement of the trend. Therefore, in order to quantify the trends, Sen's slope method (Sen, 1968) was coupled to the Mann-Kendall method. Sen's slope is used to calculate the magnitude of the trend at a given time using the gradient of the trend. The test is widely used in assessing the magnitude of the rainfall trends over time. The mathematical explanation of Sen's slope (Q_i) method is given in Equation 16.

$$Q_i = \frac{x_j - x_i}{j - i}\ for\ i = 1, \ldots\ldots, N, \tag{16}$$

where

$$Q_i = \begin{cases} Q_{\frac{N+1}{2}} & if\ N\ is\ odd \\ \dfrac{Q_{\frac{N}{2}} + Q_{\frac{N+2}{2}}}{2} & if\ N\ is\ even \end{cases}$$

The median of the N values of Q_N is symbolized as the Sen's slope estimator (Q_i) and given in the latter part of the Equation 16. Depending on the sign of the Q_i, the trend can be identified as an increasing (+ve numerical value) or decreasing (-ve numerical value) trend.

3.5. Comparison of LST and mean precipitations to NDVI values

After calculating the LST and distribution of precipitation over the forest, NDVI based relationships were established to combine the meteorological factors with forest cover area (Mao et al., 2012; Sandholt et al., 2002; Wan Mohd Jaafar et al., 2000). NDVI is a reflectance of Near Infra-Red (NIR) by plants due to photosynthesis (other rays are absorbed). Therefore, the influence of meteorological factors on vegetation can be further analyzed. The comparison studies were carried out for Land surface temperature against the NDVI and mean precipitations against the NDVI.

4. RESULTS AND DISCUSSION

4.1 Forest cover variation

The identified six land-uses and land cover classes from multiband satellite images are processed using semi-automated classification tool and presented in Figure 3 for 1992, 1997, 2005, 2016, and 2019. The differences in forest area are insignificant from these figures. However, there is a clear increase in the built-up land areas in the satellite images from 2005 to 2019, clearly shown in red color. This is interesting as they are at the boundaries of the Sinharaja Rainforest.

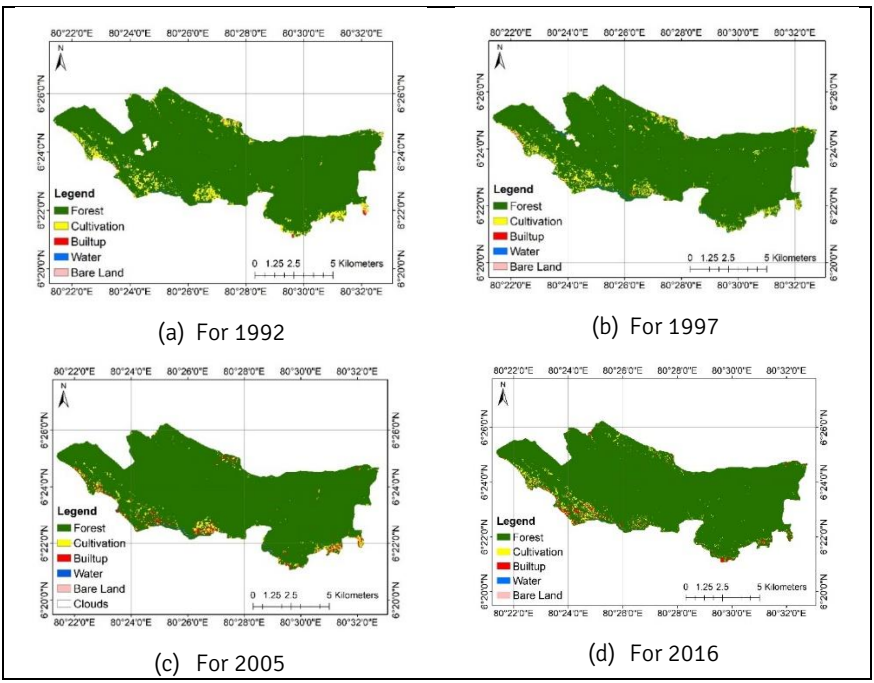

(a) For 1992

(b) For 1997

(c) For 2005

(d) For 2016

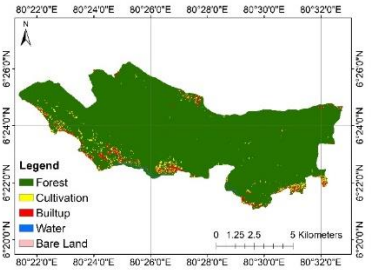

(e) For 2019

Figure 3. Land-use pattern in declared forest area

Table 2 presents the numerical analysis of the land-uses presented in Figure 3. The table reveals that the temporal variation of areas in different land-uses is dynamic over the analyzed period.

Table 2. Land use classes in the declared forest area

Land-use Class	Area (ha)					Difference in area			
	Year 1992	Year 1997	Year 2005	Year 2016	Year 2019	Δ_1	Δ_2	Δ_3	Δ_4
Forest cover	9015.21	9067.05	9212.76	9238.59	9167.04	-51.84	-145.71	-25.83	71.55
Cultivations	413.73	403.11	213.75	218.52	203.31	10.62	189.36	-4.77	15.21
Built-up areas	14.85	22.77	131.31	112.77	188.64	-7.92	-108.54	18.54	-75.87
Bare Land area	69.48	21.24	4.95	5.4	1.53	48.24	16.29	-0.45	3.87

$\Delta_1 = \Delta(1992 - 1997), \Delta_2 = \Delta(1997 - 2005), \Delta_3 = \Delta(2005 - 2016), \Delta_4 = \Delta(2016 - 2019)$
Sign convention
(-) for Gain of area compared to previous year checked
(+) for Loss of area compared to previous year checked

Interestingly, Table 2 reveals that the forest area over the years has been increased until 2016. However, there is a notable decrease in 2019 (71.55 ha). Nevertheless, there was a significant increase in forest cover from 1992 to 2019. Bare lands and cultivation lands showcase a similar trend over the years. A continuous decrease (slight exception from 2005 to 2016) in the land areas can be clearly seen from the table. The cultivated areas basically include tea, rubber plantations, and paddy fields. In-depth, cultivated areas inside the declared forest areas were reduced from 1992 – 2005. But, a heavy reduction in can be observed during 1997 – 2005.From 2005 – 2016 there was a slight increase in cultivated areas, although that was further reduced in the 2016 – 2019 period. As it was stated earlier, a similar trend was observed in the bare lands in the declared forest area. However, this was reduced entirely over time. The possible reason for reducing cultivated areas and bare lands may be due to the increase of built-up areas.

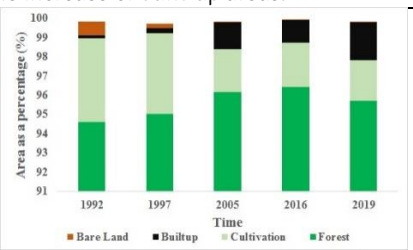

(a) Land-use class variation

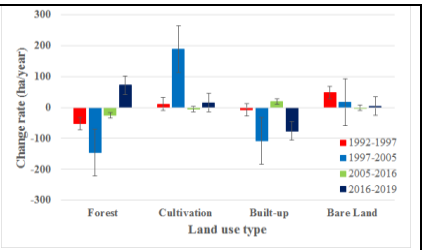

(b) Annual change rate in each land cover/use

Figure 4. Land-use class variation and rate of change in declared forest area

The built-up areas in the declared forest have been increased significantly. It was 14.85 ha in 1992; however, a steep increase to 188.64 ha has been observed. This is above 1000% of the increase over the last 28 years. The built-up areas are based on residential or commercial and tourism interest; however, a severe and continuous threat to the world heritage Sinharaja Rainforest. The continuous anthropogenic activities would further threaten the forest and bare land cover. The changes and the rate of change of land-uses can be further observed in Figure 4. This clearly shows the overtaking of the bare land areas to the built-up areas.

4.2 NDVI for Sinharaja forest

The previous section summarizes an increase in forest cover from 1992 to 2016, and it was then suddenly decreased from 2016 to 2019. Therefore, it is interesting to understand the influence of climate change on these forest cover changes. Thus, the NDVI was calculated for each year. Figure 5 presents the distribution of NDVI for the years 1992, 1995, 1997, 2005, 2016, and 2019. The darker the colour (green), the forest is denser.

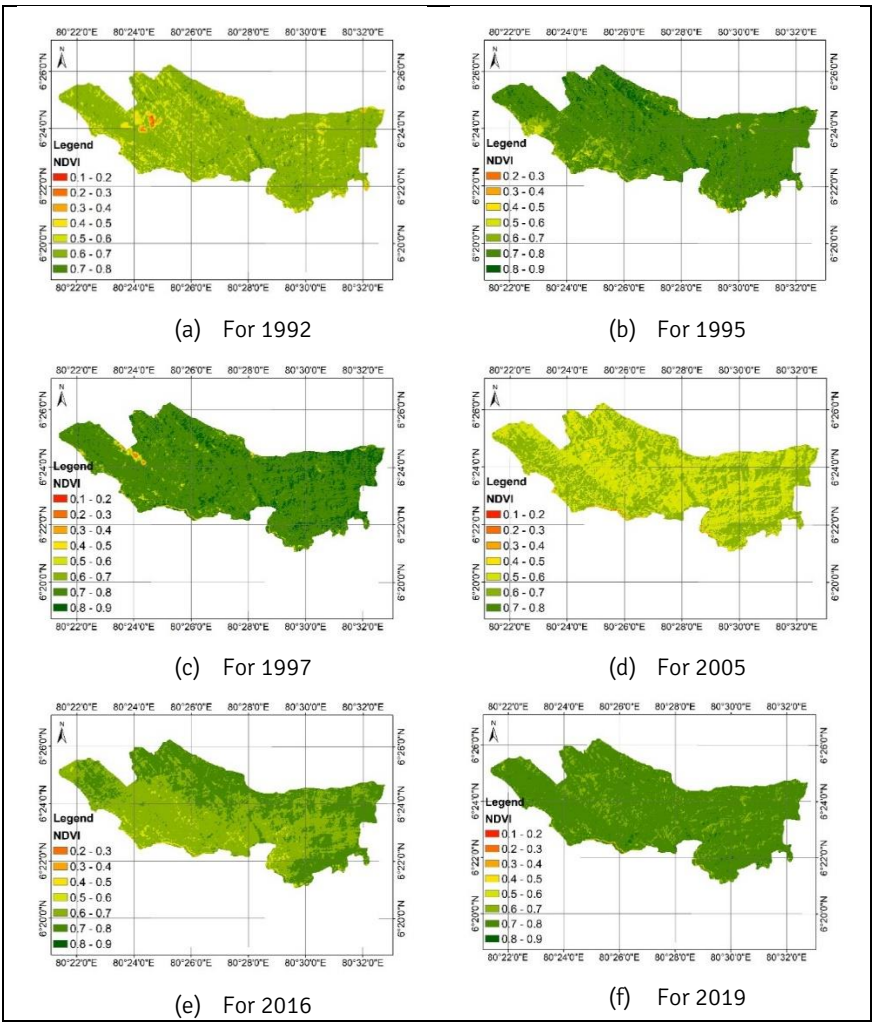

Figure 5. NDVI distribution over the time

Figures 5a-5f show some interesting variations in colour even though these Landsat images were captured on average at the same time of the year (February-March-April). Therefore, the usual climate patterns can be expected to constrain all of these NDVI values. The years 1992, 1995, and 2019 showcase some thick or healthier forest cover across the Sinharaja Rainforest. However, the years 1992 and 2005 have low denser forest cover, and this could be due to some dry weather conditions in the area. This observation can be further discussed based on the numerical basis of the NDVIs, which are given in Table 3. It shows the NDVI values ranging from 0 – 0.9 and the forest area coverage (in hectares). NDVI values greater than 0.5 are usually considered healthy forest covers.

Table 3. NDVI values and area of forest

NDVI Value	Area in (ha)					
	1992	1995	1997	2005	2016	2019
0.1-0.2	1.53	0	0.27	3.51	0	0.72
0.2-0.3	18.45	0.63	9.90	9.45	0.18	2.88
0.3-0.4	39.42	7.38	18.63	22.68	4.41	6.57
0.4-0.5	146.88	24.57	30.51	298.53	19.98	9.54
0.5-0.6	1298.70	117.90	81.45	4974.21	251.91	27.00
0.6-0.7	7721.82	794.34	385.29	4266.36	5366.88	883.98
0.7-0.8	353.34	7953.39	7745.49	5.40	3932.91	8584.38
0.8-0.9	0	681.93	1308.60	0	3.87	65.07

Compared to the year 1992, NDVI values of the year 1995 for Sinharaja Rainforest were significantly changed. The NDVI range was increased from 0.6 – 0.7 to 0.7 – 0.8 (353.34 to 7953.39 ha). The increase of NDVI means the forest cover becomes healthier, greener, and mature (which can be seen in Figure 5b). Furthermore, it is observed that the forest area with 0.8 – 0.9 (Denser and Mature) range improved by approximately twice of 1995 in 1997. However, in 2005 most of the areas with higher NDVI values in 1997 were reduced. But, in the 2016 – 2019 period compared to 2005, the NDVI ranges again improved.

As it is well understood, there can be some unauthorized cultivated areas inside the Sinharaja Rainforest. This can be validated by in-depth field surveys.

4.3 LST variation

LST variation over time was obtained using the remotely sensed LST retrieved from the Land satellite images. However, before any further analysis, the remotely sensed LSTs, based on the empirical formulas, were validated based on the measured LST at the Faculty of Agriculture, University of Ruhuna, Sri Lanka. The comparison showed an acceptable agreement (R2 = 0.92) between the empirically calculated LST and measured LST, even though some fluctuations could be observed in cloud-covered areas. Figure 6 shows the comparison of measured and empirically calculated LST. On average the empirically calculated LSTs were numerically higher than the measured LSTs. However, there are two outliers, where the difference between the measured and empirical LSTs is 7.15 0C and this was on 07/04/1995. In addition, another outlier can be seen on 28/02/2016, which is about 2.78 0C indifference.

With these acceptable validations, the LST values from satellite images were further used to compare. The six sites shown in Figure 2 were carefully identified as the deforested area without human influence, and the authors believed these have happened solely due to environmental impacts. The LST analysis was initially carried out to these six sites and then, to the entire forest area. An increasing trend in LST was observed with some fluctuations for the six selected sites presented in Figures. 7 and 8.

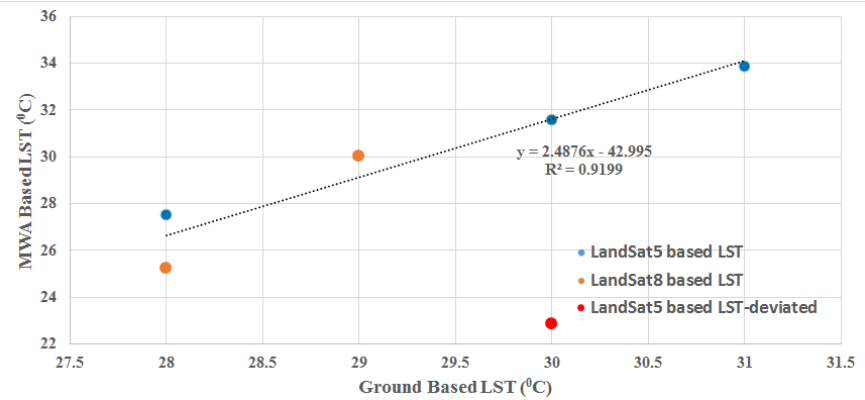

Figure 6. Measured LST against empirical LST

Table 4. LST and NDVI variation of deforested areas

Year	LST (°c)						NDVI					
	LC1	LC2	LC3	LC4	LC5	LC6	LC1	LC2	LC3	LC4	LC5	LC6
1992	30.3	28.3	28.3	27.6	26.4	26.0	0.59	0.63	0.65	0.54	0.62	0.37
1995	19.2	18.2	18.3	18.6	17.7	16.5	0.78	0.51	0.80	0.62	0.73	0.53
1997	22.4	21.0	25.2	24.2	23.5	23.0	0.61	0.69	0.66	0.67	0.73	0.60
2005	27.0	26.3	25.4	26.7	27.3	23.9	0.55	0.58	0.64	0.55	0.56	0.46
2016	23.4	22.7	22.8	22.3	19.9	20.9	0.73	0.72	0.75	0.65	0.49	0.54
2019	25.3	26.5	26.9	27.0	26.6	24.7	0.76	0.57	0.74	0.65	0.61	0.60

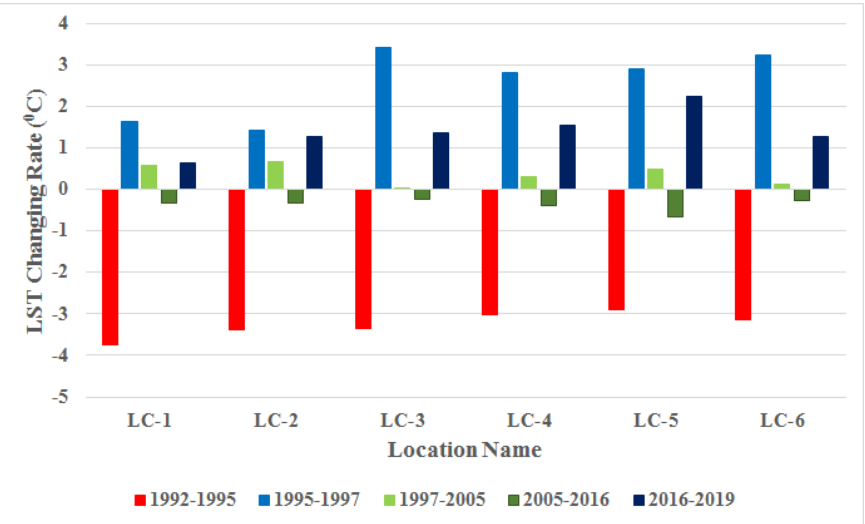

Figure 7. LST Change rates at six locations

All LSTs in 1992 showcased high values; then, reduced in 1996. The sites LC1, LC2, and LC3 are close to each other (can be seen from Figure 2). Therefore, LC1 and LC2 sites showed similar behaviour of LST variations and change rates. Based on the LSTs shown in Table 4, it can be clearly seen that the year 1995 is a slightly cooler year compared to others. The LST change rates are comparably high from 1992 to 1995 (negative) and from 1995 to 1997 (positive). However, these LST rates are milder for the other year intervals. These are clearly observed from Figure 7. However, there was a notable rate of increase in LST for LC5 during 2016 -2019. Therefore, combining all

these observations, the authors would happy to propose a milder upward LST trend in the Sinharaja rainforest. Nevertheless, more research has to be carried out continuously for sound conclusions. In addition, the NDVI values for these six locations over the years can be seen from the Table 7. The values do not showcase drastic changes but slight temporal changes can be observed.

Figure 8 presents LSTs' temporal and spatial variation for the entire forest area. Figure 8a showcases the LST variation to 1992. It can be clearly seen that the LSTs are comparably higher than in other years. LSTs above 35 0C are shown in red patches. These patches are visible in the forest's northern and south-eastern boundary not shown in significant areas. The average LST is in the range of 25-30 0C. However, interesting features in LST can be found in the year 1995. The land surface of the whole forest area has cooler temperatures and the range is in between 10-15 0C. Nevertheless, the LSTs were increased and reached 25-30 0C except in 2016.

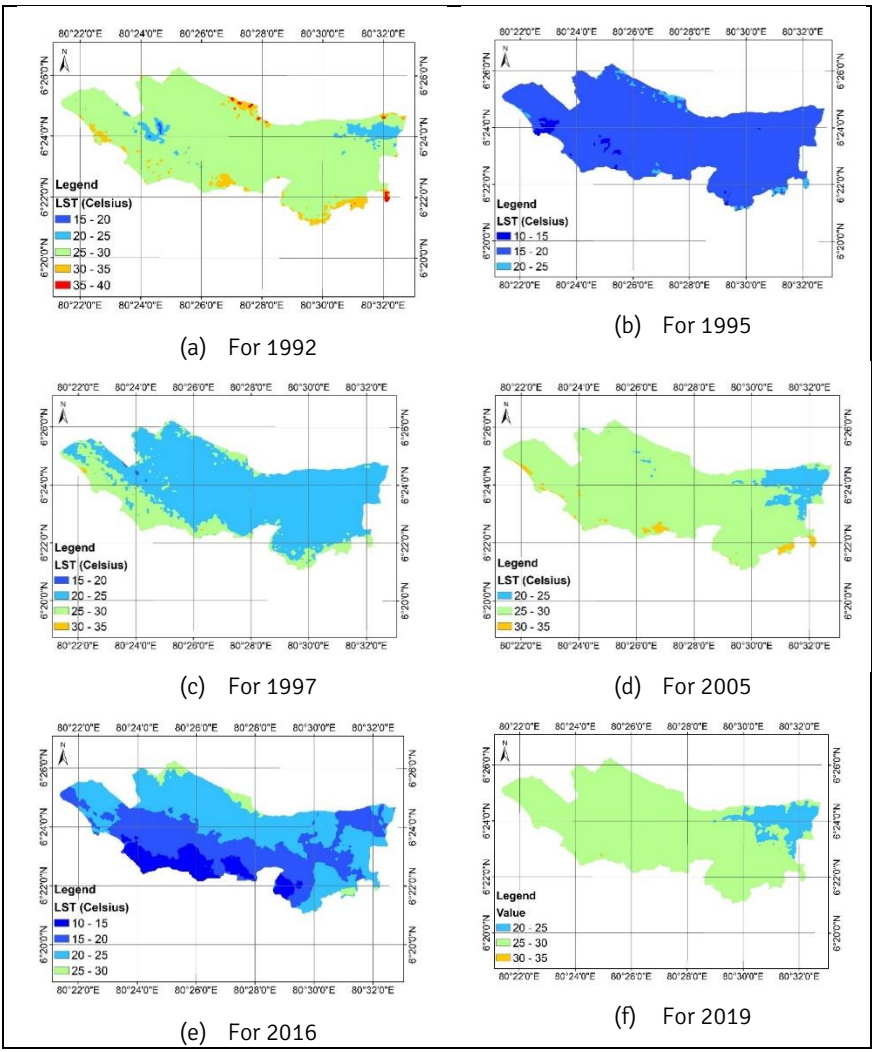

Figure 8. LST variation at Sinharaja Rainforest

4.4 Rainfall trend analysis and spatial distribution of rainfall

Possible rainfall trends to the measured rainfall were carried out using Mann-Kendall and Sen's slope estimator tests for the Kudawa, Deniyaya, Pallegamathanna, Pelawatta, and Depedena rainfall stations. None of the stations showcase a positive or negative rainfall trend over the last 30 years. Deniyaya showed a negative rainfall trend; however, it can be considered an insignificant trend due to the magnitude of the trend (-0.00614 mm/year). The temporal and spatial variations for the rainfall inside the Sinharaja Rainforest cannot be identified from the measured rainfalls.

The spatial distribution of rainfall is important for further study on forest cover. Therefore, the inverse distance weight interpolation method was used to identify the distribution of precipitation in the forest area. The satellite images were used in these findings; however, the accumulated rainfall from the previous year was considered. Figure 9 showcases rainfall's spatial and temporal variation inside the Sinharaja Rainforest area.

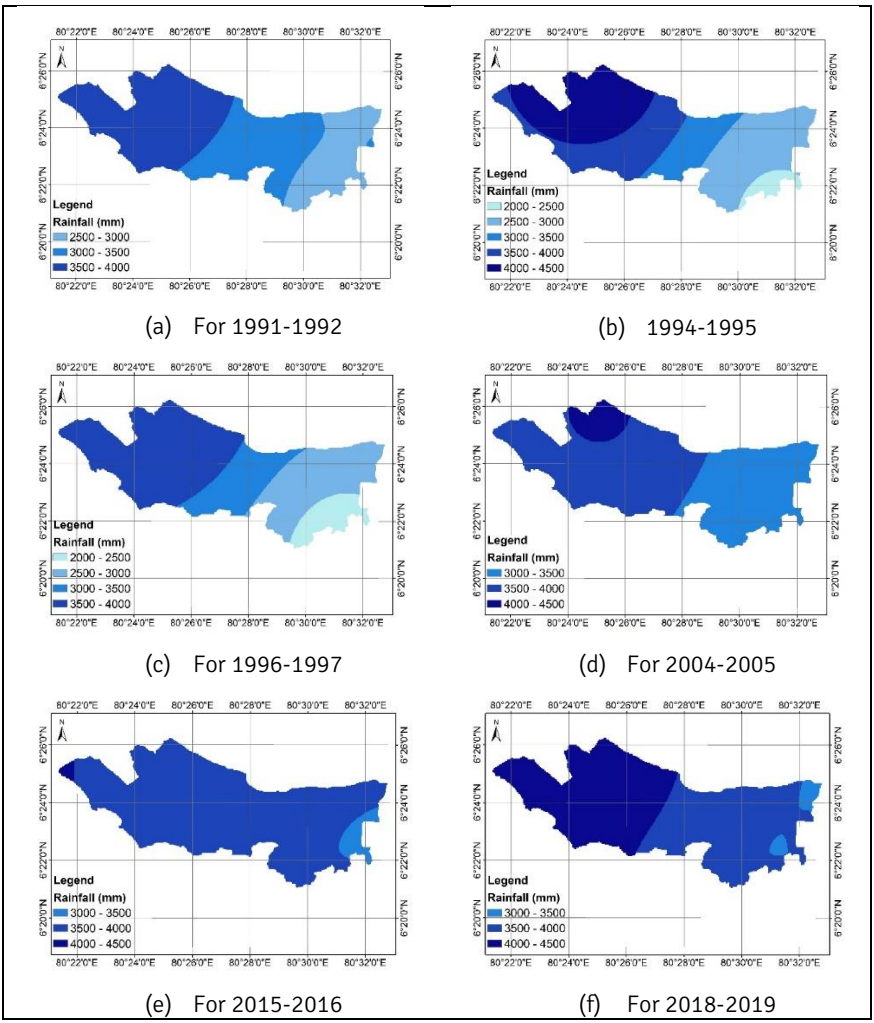

Figure 9. Spatial and temporal distribution of rainfall

Mean precipitation distribution for the 1991 – 1992 year is quite low compared to the year 1994 – 1995 period. More annual rain may improve the growth of the vegetation. However, approximately a similar trend was observed in the 1996 – 1997 period compared to 1991 -1992. During the 2004 – 2005 period the accumulated rainfall over the forest was increased and the entire forest received over 3000 mm rainfall. For the rest of the years, the spatial distribution of rainfall shows that most areas received more than 3000 mm of accumulated rainfall and some have received more than 3500 mm of rainfalls. Furthermore, above 4000 mm rainfalls can be seen in 2018-2019.

4.5 Relationship between NDVI and LST

Sandholt et al. (2002) have shown that the NDVI and LST values have negative linear correlation (but insignificant) and the establishment of the dryline (expected trends in Figure 10, dashed lines). That approach was directly applied to understand the NDVI and LST correlation at Sinharaja Rainforest. Figure 10 shows the LST variation with respect to the NDVI variation and dry areas and wet areas are shown in the figure.

Figure 8a shows a high LST distribution over the entire forest for the year 1992. This observation has entirely affected the NDVI distribution in the forest area. NDVI values for 1992 (red dots) are above the corresponding dryline (red dashed line) for NDVI values of 0.5-1 in Figure 10. That means no or less transpiration took place during the year 1992 and thus, resulted in a moderately healthy forest cover.

However, in 1995 – 1997 majority of the points of NDVI lie in the wet wedge. Therefore, transpiration evaporation and ecological processes work effectively and result in healthy and increased forest cover. But for the years 2005, 2016, and 2019 most of the NDVI values representing the forest vegetation lie above the expected dry lines. Therefore, the increase of forest cover is considerably minimized. Further, it is observed an increase in LST from 2005 – 2019 at high NDVI locations, and that can adversely impact flora and fauna required lower temperatures.

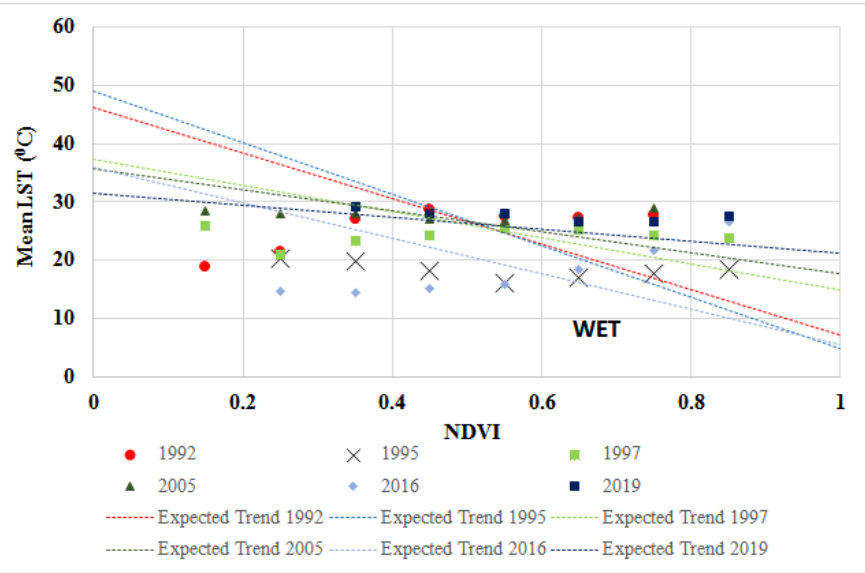

Figure 10. LST variation with respect to NDVI

4.6 Relationship between NDVI and precipitation

Wan Mohd Jaafar et al. (2020) and Mao et al. (2012) have shown that NDVI and precipitation have a positive but significant linear correlation based on their findings. Figure 11 exhibits the relationship between precipitation and NDVI for Sinharaja Rainforest. A boundary line was established for the precipitation similar to the previous section (section, Relationship between NDVI and LST, dashed line) and plotted the mean precipitation with respect to NDVI (refer Figure 11).

In general, no significant rainfall trends were observed in most of the highly vegetated areas (i.e., High in NDVI Value). The accumulated precipitation of years 1991-1992 was reduced in highly vegetated areas. However, most of the forest places received high precipitation, which was the reason to have a high forest area with healthy vegetation. Nevertheless, in 2005, the precipitation lies below the boundary line at highly vegetated areas and becomes the reason for having a less healthy forest cover. However, the accumulated precipitation for 2015 – 2016 is almost parallel to the boundary line and that might be the reason for improving NDVI values of the forest compared to 2005. The 2019 event is a special as the accumulated rainfall reaches its highest compared to other years. Even though most of the NDVI regions received less precipitation compared to expect. But the magnitude might be the reason for the increase of the greenish colour of the forest and make it healthier. Therefore, the relationship between NDVI and precipitation is justified.

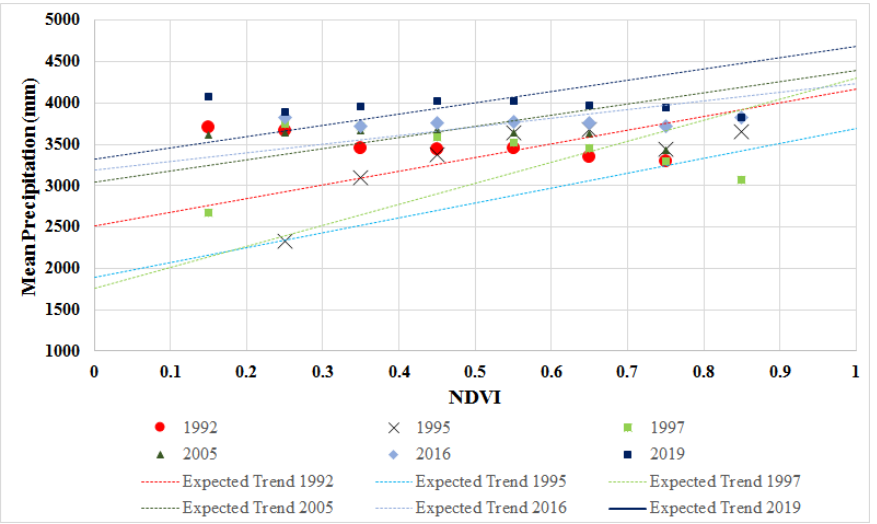

Figure 11. Mean precipitation and NDVI variation

5. CONCLUSION

This paper presents a timely important discussion on the impact of climate change on the World Heritage Rainforest; Sinharaja in Sri Lanka. The discussion extended to the human activities in the vicinity and declared forest areas as built-up areas. Land-use patterns, Land Surface Temperatures, Normalized Difference Vegetation Index, and rainfall trend analysis were combined to identify any potential climate change impacts to the Sinharaja Rainforest. The interaction of each parameter is tested.

Land-use pattern analysis clearly presented the increase of built-in areas in the vicinity of the declared forest areas over time. Therefore, it can be concluded that a growing threat is there to the nation's pride; Sinharaja Rainforest. This finding will benefit all stakeholders and then impose enough rules and regulations to control the

new built-up areas in the declared forest area. In addition, the rules and regulations should be brought up to manage the established built-up areas.

Higher rainfalls in the western parts of the forest compared to the eastern parts can be observed from spatial distribution of the rainfall over the years. However, no rainfall trend was identified using the well-known non-parametric tests. Therefore, there is no critical concern about the rainfall received in the Sinharaja forest. In addition, the healthiness of the forest cover was well established from the LST to NDVI variation and the mean precipitation to NDVI variation. The spatial distribution of the LST concludes higher temperatures in the northern and southern boundaries of the forest. Many development activities can be seen over the years in the vicinity of the forest. Nevertheless, the LST to NDVI relationship justified the forest cover variation to the whole Sinharaja Rainforest. The variations concluded that the forest cover increase is minimal temporally compared to early years (1992 – 1997). Mean precipitation to NDVI variation concludes the decreasing rainfall trend in the high NDVI areas. Therefore, the forest cover is heading to dry in high precipitation areas. However, the forest area has regained the greenish color in the latter years. Therefore, the research clearly showcases the importance of such a study for the first time in Sri Lanka, which is the most important forest; Sinharaja Rainforest!

Author Contributions: Author 1; Methodology, investigation, visualization and writing the original draft: Author 2; Methodology and writing the original draft: Author 3; Methodology and investigation: Author 4; Methodology and investigation: Author 5; Conceptualization, supervision, reviewing the writing, and editing the finalized manuscript.

Competing Interests: The authors declare that they have no competing interests.

Acknowledgments: The authors would like to acknowledge the support received from Sri Lanka Institute of Information of Technology to carry out this research work.

REFERENCES

Anderson, M. C., Allen, R. G., Morse, A., & Kustas, W. P. (2012). Use of Landsat thermal imagery in monitoring evapotranspiration and managing water resources. *Remote Sensing of Environment, 122,* 50-65. https://doi.org/10.1016/j.rse.2011.08.025

Athick, A. M. A., Shankar, K., & Naqvi, H. R. (2019). Data on time series analysis of land surface temperature variation in response to vegetation indices in twelve Wereda of Ethiopia using mono window, split window algorithm and spectral radiance model. *Data in brief, 27,* 104773. https://doi.org/10.1016/j.dib.2019.104773

Baker, J. R. (1937). The Sinharaja Rain-Forest, Ceylon. *The Geographical Journal, 89*(6), 539–551. https://doi.org/10.2307/1787913

Bebi, P., Seidl, R., Motta, R., Fuhr, M., Firm, D., Krumm, F., Conedera, M., Ginzler, C., Wohlgemuth, T. and Kulakowski, D. (2017). Changes of forest cover and disturbance regimes in the mountain forests of the Alps. *Forest ecology and management, 388,* 43–56. https://doi.org/10.1016/j.foreco.2016.10.028

Benchimol, M., & Peres, C. A. (2015). Widespread forest vertebrate extinctions induced by a mega hydroelectric dam in lowland Amazonia. *PloS one, 10*(7), e0129818. https://doi.org/10.1371/journal.pone.0129818

Birhane, E., Ashfare, H., Fenta, A. A., Hishe, H., Gebremedhin, M. A., G. Wahed, H., & Solomon, N. (2019). Land use land cover changes along topographic gradients in Hugumburda national forest priority area, Northern Ethiopia. *Remote Sensing Applications: Society and Environment, 13,* 61–68. https://doi.org/10.1016/j.rsase.2018.10.017

Chatterjee, R. S., Singh, N., Thapa, S., Sharma, D., & Kumar, D. (2017). Retrieval of land

surface temperature (LST) from landsat TM6 and TIRS data by single channel radiative transfer algorithm using satellite and ground-based inputs. *International journal of applied earth observation and geoinformation, 58,* 264-277. https://doi.org/10.1016/j.jag.2017.02.017

Chen, H., Chandrasekar, V., Cifelli, R., & Xie, P. (2019). A machine learning system for precipitation estimation using satellite and ground radar network observations. *IEEE Transactions on Geoscience and Remote Sensing, 58*(2), 982-994. https://doi.org/10.1109/TGRS.2019.2942280

Choi, S., Lee, W. K., Kwak, D. A., Lee, S., Son, Y., Lim, J. H., & Saborowski, J. (2011). Predicting forest cover changes in future climate using hydrological and thermal indices in South Korea. *Climate Research, 49*(3), 229-245. https://doi.org/10.3354/cr01026

Congedo, L. (2016). Semi-automatic classification plugin documentation. *Release, 4*(0.1), 29. https://doi.org/10.21105/joss.03172

Cristóbal, J., Jiménez-Muñoz, J. C., Prakash, A., Mattar, C., Skoković, D., & Sobrino, J. A. (2018). An improved single-channel method to retrieve land surface temperature from the Landsat-8 thermal band. *Remote Sensing, 10*(3), 431. https://doi.org/10.3390/rs10030431

Dash, P., Göttsche, F. M., Olesen, F. S., & Fischer, H. (2001). Retrieval of land surface temperature and emissivity from satellite data: physics, theoretical limitations and current methods. *Journal of the Indian Society of Remote Sensing, 29*(1), 23-30. https://doi.org/10.1007/BF02989910

De Silva, R. P., Dayawansa, N. D. K., & Ratnasiri, M. D. (2007). A comparison of methods used in estimating missing rainfall data. *The Journal of Agricultural Sciences, 3*(2), 101-108. https://doi.org/10.4038/jas.v3i2.8107

Fokeng, R. M., Forje, W. G., Meli, V. M., & Bodzemo, B. N. (2020). Multi-temporal forest cover change detection in the Metchie-Ngoum protection forest reserve, West Region of Cameroon. *The Egyptian Journal of Remote Sensing and Space Science, 23*(1), 113-124. https://doi.org/10.1016/j.ejrs.2018.12.002

García-Santos, V., Cuxart, J., Martínez-Villagrasa, D., Jiménez, M. A., & Simó, G. (2018). Comparison of three methods for estimating land surface temperature from landsat 8-tirs sensor data. *Remote Sensing, 10*(9), 1450. https://doi.org/10.3390/rs10091450

Gibbs, H. K., Ruesch, A. S., Achard, F., Clayton, M. K., Holmgren, P., Ramankutty, N., & Foley, J. A. (2010). Tropical forests were the primary sources of new agricultural land in the 1980s and 1990s. *Proceedings of the National Academy of Sciences, 107*(38), 16732–16737. https://doi.org/10.1073/pnas.0910275107

Gunathilake, N., De Mel, T., De Mel, W. C. P., Sheriff, M. H. R., & Dharmadasa, K. (1987). The value of the use of renal function indices in distinguishing prerenal failure from established acute oliguric renal failure.

Gunatilleke, S., Gunatilleke, I., Sheppard, D., Sax, J., Forster, M., Hoffmann, T., Fernando, V., Synge, H., Edisvik, H., De Zoysa, N., Fernando, R. & Forest Dept. Staff. (1987). Sinharaja Forest Reserve (Sri Lanka), World Heritage Nomination - IUCN Summary, 405, 67-71.

Hansen, M. C., Potapov, P. V., Moore, R., Hancher, M., Turubanova, S. A., Tyukavina, A., ... & Townshend, J. (2013). High-resolution global maps of 21st-century forest cover change. *Science, 342*(6160), 850-853. https://doi.org/10.1126/science.1244693

Härkönen, S., Neumann, M., Mues, V., Berninger, F., Bronisz, K., Cardellini, G., ... & Mäkelä, A. (2019). A climate-sensitive forest model for assessing impacts of forest management in Europe. *Environmental Modelling & Software, 115,* 128-143.

https://doi.org/10.1016/j.envsoft.2019.02.009

Haylock, M. R., Hofstra, N., Klein Tank, A. M. G., Klok, E. J., Jones, P. D., & New, M. (2008). A European daily high-resolution gridded data set of surface temperature and precipitation for 1950–2006. *Journal of Geophysical Research: Atmospheres, 113*(D20). https://doi.org/10.1029/2008JD010201

Heartsill-Scalley, T., & Aide, T. M. (2003). Riparian vegetation and stream condition in a tropical agriculture–secondary forest mosaic. *Ecological Applications, 13*(1), 225-234. https://doi.org/10.1890/1051-761(2003)013[0225:RVASCI]2.0.CO;2

Hirsch, R. M., & Slack, J. R. (1984). A nonparametric trend test for seasonal data with serial dependence. *Water Resources Research, 20*(6), 727-732. https://doi.org/10.1029/WR020i006p00727

Huang, C., Kim, S., Song, K., Townshend, J. R., Davis, P., Altstatt, A., ... & Musinsky, J. (2009). Assessment of Paraguay's forest cover change using Landsat observations. *Global and Planetary Change, 67*(1-2), 1-12. https://doi.org/10.1016/j.gloplacha.2008.12.009

Ji, W., Wang, Y., Zhuang, D., Song, D., Shen, X., Wang, W., & Li, G. (2014). Spatial and temporal distribution of expressway and its relationships to land cover and population: A case study of Beijing, China. *Transportation Research Part D: Transport and Environment, 32,* 86-96. https://doi.org/10.1016/j.trd.2014.07.010

Jin, X., & Davis, C. H. (2007). Vehicle detection from high-resolution satellite imagery using morphological shared-weight neural networks. *Image and Vision Computing, 25*(9), 1422-1431. https://doi.org/10.1016/j.imavis.2006.12.011

Karmeshu, N. (2012). *Trend detection in annual temperature & precipitation using the Mann Kendall test-a case study to assess climate change on select states in the northeastern United States* [Master Thesis]. University of Pennsylvania.

Karnieli, A., Agam, N., Pinker, R. T., Anderson, M., Imhoff, M. L., Gutman, G. G., ... & Goldberg, A. (2010). Use of NDVI and land surface temperature for drought assessment: Merits and limitations. *Journal of climate, 23*(3), 618-633. https://doi.org/10.1175/2009JCLI2900.1

Khan, S. H., He, X., Porikli, F., & Bennamoun, M. (2017). Forest change detection in incomplete satellite images with deep neural networks. *IEEE Transactions on Geoscience and Remote Sensing, 55*(9), 5407-5423. https://doi.org/10.1109/TGRS.2017.2707528

Khaniya, B., Jayanayaka, I., Jayasanka, P., & Rathnayake, U. (2019). Rainfall trend analysis in Uma Oya basin, Sri Lanka, and future water scarcity problems in perspective of climate variability. Advances in Meteorology, 2019. https://doi.org/10.1155/2019/3636158

Kim, S. R., Lee, W. K., Kwak, D. A., Biging, G. S., Gong, P., Lee, J. H., & Cho, H. K. (2011). Forest cover classification by optimal segmentation of high resolution satellite imagery. *Sensors, 11*(2), 1943-1958. https://doi.org/10.3390/s110201943

Kislov, D. E., Korznikov, K. A., Altman, J., Vozmishcheva, A. S., & Krestov, P. V. (2021). Extending deep learning approaches for forest disturbance segmentation on very high-resolution satellite images. *Remote Sensing in Ecology and Conservation, 7*(3), 355-368. https://doi.org/10.1002/rse2.194

Labbi, A., & Mokhnache, A. (2015). Derivation of split-window algorithm to retrieve land surface temperature from MSG-1 thermal infrared data. *European Journal of Remote Sensing, 48(*1), 719-742. https://doi.org/10.5721/EuJRS20154840

Leach, M. and Fairhead, J. (2000). Challenging neo-Malthusian deforestation analyses in West Africa's dynamic forest landscapes. *Population and Development Review, 26,* 17–43. https://doi.org/10.1111/j.1728-4457.2000.00017.x

Leimgruber, P., Kelly, D. S., Steininger, M. K., Brunner, J., Müller, T., & Songer, M. (2005). Forest cover change patterns in Myanmar (Burma) 1990–2000. *Environmental Conservation, 32*(4), 356-364. https://doi.org/10.1017/S0376892905002493

Lindström, S., Mattsson, E., & Nissanka, S. P. (2012). Forest cover change in Sri Lanka: The role of small scale farmers. *Applied Geography, 34,* 680-692. https://doi.org/10.1016/j.apgeog.2012.04.011

Mann, H. B. (1945). Nonparametric tests against trend. *Econometrica: Journal of the econometric society, 13*(3) 245-259. https://doi.org/10.2307/1907187

Mao, D., Wang, Z., Luo, L., & Ren, C. (2012). Integrating AVHRR and MODIS data to monitor NDVI changes and their relationships with climatic parameters in Northeast China. *International Journal of Applied Earth Observation and Geoinformation, 18,* 528-536. https://doi.org/10.1016/j.jag.2011.10.007

Margono, B. A., Potapov, P. V., Turubanova, S., Stolle, F., & Hansen, M. C. (2014). Primary forest cover loss in Indonesia over 2000–2012. *Nature climate change, 4*(8), 730-735. https://doi.org/10.1038/nclimate2277

Matricardi, E. A., Skole, D. L., Pedlowski, M. A., Chomentowski, W., & Fernandes, L. C. (2010). Assessment of tropical forest degradation by selective logging and fire using Landsat imagery. *Remote Sensing of Environment, 114*(5), 1117-1129. https://doi.org/10.1016/j.rse.2010.01.001

Mujabar, S., & Rao, V. (2018). Estimation and analysis of land surface temperature of Jubail Industrial City, Saudi Arabia, by using remote sensing and GIS technologies. *Arabian Journal of Geosciences, 11*(23), 1-13. https://doi.org/10.1007/s12517-018-4109-y

Perera, K., & Tsuchiya, K. (2009). Experiment for mapping land cover and it's change in southeastern Sri Lanka utilizing 250 m resolution MODIS imageries. *Advances in Space Research, 43*(9), 1349-1355. https://doi.org/10.1016/j.asr.2008.12.016

Peterson, C. J. (2000). Catastrophic wind damage to North American forests and the potential impact of climate change. *Science of the Total Environment, 262*(3), 287-311. https://doi.org/10.1016/S0048-9697(00)00529-5

Qin, Z., Karnieli, A., & Berliner, P. (2001). A mono-window algorithm for retrieving land surface temperature from Landsat TM data and its application to the Israel-Egypt border region. *International journal of remote sensing, 22*(18), 3719-3746. https://doi.org/10.1080/01431160010006971

Ranagalage, M., Gunarathna, M. H. J. P., Surasinghe, T. D., Dissanayake, D., Simwanda, M., Murayama, Y., ... & Sathurusinghe, A. (2020). Multi-decadal forest-cover dynamics in the tropical realm: Past trends and policy insights for forest conservation in dry zone of Sri Lanka. *Forests, 11*(8), 836. https://doi.org/10.3390/f11080836

Rathnayake, C. W., Jones, S., & Soto-Berelov, M. (2020). Mapping land cover change over a 25-year period (1993–2018) in Sri Lanka using Landsat time-series. *Land, 9*(1), 27. https://doi.org/10.3390/land9010027

Rathnayake, U. (2019). Comparison of statistical methods to graphical methods in rainfall trend analysis: case studies from tropical catchments. *Advances in Meteorology*, 2019. https://doi.org/10.1155/2019/8603586

Rongali, G., Keshari, A. K., Gosain, A. K., & Khosa, R. (2018). Split-window algorithm for retrieval of land surface temperature using Landsat 8 thermal infrared data. Journal of Geovisualization and Spatial *Analysis, 2*(2), 1-19. https://doi.org/10.1007/s41651-018-0021-y

Sahin, S., & Cigizoglu, H. K. (2010). Homogeneity analysis of Turkish meteorological data set. Hydrological Processes: *An International Journal, 24*(8), 981-992. https://doi.org/10.1002/hyp.7534

Sandholt, I., Rasmussen, K., & Andersen, J. (2002). A simple interpretation of the surface temperature/vegetation index space for assessment of surface moisture status. *Remote Sensing of environment, 79(*2-3), 213-224. https://doi.org/10.1016/S0034-4257(01)00274-7

Sekertekin, A., & Bonafoni, S. (2020). Land surface temperature retrieval from Landsat 5, 7, and 8 over rural areas: Assessment of different retrieval algorithms and emissivity models and toolbox implementation. *Remote Sensing, 12*(2), 294. https://doi.org/10.3390/rs12020294

Sen, P. K. (1968). Estimates of the regression coefficient based on Kendall's tau. *Journal of the American statistical association, 63*(324), 1379-1389. https://doi.org/10.1080/01621459.1968.10480934

Sirisena, D., & Suriyagoda, L. D. (2018). Toward sustainable phosphorus management in Sri Lankan rice and vegetable-based cropping systems: A review. *Agriculture and Natural Resources, 52*(1), 9-15. https://doi.org/10.1016/j.anres.2018.03.004

Sobrino, J. A., Jiménez-Muñoz, J. C., Sòria, G., Romaguera, M., Guanter, L., Moreno, J., Plaza, A. & Martínez, P. (2008). Land surface emissivity retrieval from different VNIR and TIR sensors. *IEEE transactions on geoscience and remote sensing, 46*(2), 316-327. https://doi.org/10.1109/TGRS.2007.904834

Song, W., Mu, X., Ruan, G., Gao, Z., Li, L., & Yan, G. (2017). Estimating fractional vegetation cover and the vegetation index of bare soil and highly dense vegetation with a physically based method. *International journal of applied earth observation and geoinformation, 58*, 168-176. https://doi.org/10.1016/j.jag.2017.01.015

Stibig, H. J., & Malingreau, J. P. (2003). Forest cover of insular Southeast Asia mapped from recent satellite images of coarse spatial resolution. *AMBIO: A Journal of the Human Environment, 32(7*), 469-475. https://doi.org/10.1579/0044-7447-32.7.469

Sun, L., Liu, X., Yang, Y., Chen, T., Wang, Q., & Zhou, X. (2018). A cloud shadow detection method combined with cloud height iteration and spectral analysis for Landsat 8 OLI data. *ISPRS Journal of Photogrammetry and Remote Sensing, 138*, 193-207. https://doi.org/10.1016/j.isprsjprs.2018.02.016

Sy, S., & Quesada, B. (2020). Anthropogenic land cover change impact on climate extremes during the 21st century. *Environmental Research Letters, 15*(3), 034002. https://doi.org/10.1088/1748-9326/ab702c

Sylvain, J. D., Drolet, G., & Brown, N. (2019). Mapping dead forest cover using a deep convolutional neural network and digital aerial photography. *ISPRS Journal of Photogrammetry and Remote Sensing, 156,* 14-26. https://doi.org/10.1016/j.isprsjprs.2019.07.010

Temudo, M. P., & Silva, J. M. (2012). Agriculture and forest cover changes in post-war Mozambique. *Journal of Land Use Science, 7*(4), 425-442. https://doi.org/10.1080/1747423X.2011.595834

van Leeuwen, T. T., Frank, A. J., Jin, Y., Smyth, P., Goulden, M. L., van der Werf, G. R., & Randerson, J. T. (2011). Optimal use of land surface temperature data to detect changes in tropical forest cover. *Journal of Geophysical Research: Biogeosciences, 116*(G2). https://doi.org/10.1029/2010JG001488

Viana, C. M., Oliveira, S., Oliveira, S. C., & Rocha, J. (2019). Land use/land cover change detection and urban sprawl analysis. In Spatial modeling in GIS and R for earth and environmental sciences. In Pourghasemi, H. R. & Gokceoglu, C. (Eds.), *Spatial Modeling in GIS and R for Earth and Environmental Sciences* (pp. 621-651). Elsevier. https://doi.org/10.1016/B978-0-12-815226-3.00029-6

Walthert, L., Pannatier, E. G., & Meier, E. S. (2013). Shortage of nutrients and excess of toxic elements in soils limit the distribution of soil-sensitive tree species in

temperate forests. *Forest ecology and management, 297,* 94-107. https://doi.org/10.1016/j.foreco.2013.02.008

Wan Mohd Jaafar, W. S., Abdul Maulud, K. N., Muhmad Kamarulzaman, A. M., Raihan, A., Md Sah, S., Ahmad, A., Saad, S.N.M., Ahmad Tarmizi Mohd Azmi, A.T.M., Syukri, N.K.A.J. & Razzaq Khan, W. (2020). The influence of deforestation on land surface temperature—a case study of Perak and Kedah, Malaysia. *Forests, 11*(6), 670. https://doi.org/10.3390/f11060670

Wang, F., Fan, W., Lin, X., Liu, J. and Ye, X. (2020). Does population mobility contribute to urbanization convergence? Empirical evidence from three major urban agglomerations in China. *Sustainability. 12*(2), 458. https://doi.org/10.3390/su12020458

Wang, M., Zhang, Z., He, G., Wang, G., Long, T., & Peng, Y. (2016). An enhanced single-channel algorithm for retrieving land surface temperature from Landsat series data. *Journal of Geophysical Research: Atmospheres, 121*(19), 11-712. https://doi.org/10.1002/2016JD025270

Yu, X., Guo, X., & Wu, Z. (2014). Land surface temperature retrieval from Landsat 8 TIRS—Comparison between radiative transfer equation-based method, split window algorithm and single channel method. *Remote sensing, 6*(10), 9829-9852. https://doi.org/10.3390/rs6109829

Zhang, R., Zhao, X., Zhang, C., & Li, J. (2020). Impact of rapid and intensive land use/land cover change on soil properties in arid regions: a case study of Lanzhou new area, China. *Sustainability, 12*(21), 9226. https://doi.org/10.3390/su12219226

Zhu, Z., & Waller, E. (2003). Global forest cover mapping for the United Nations Food and Agriculture Organization forest resources assessment 2000 program. *Forest science, 49*(3), 369-380. https://doi.org/10.1093/forestscience/49.3.369